Methodological approach for trace and essential elements assessment in prostate tissue by SRIXE method

Bohdan Pawlicki[1], Aleksandra Pawlicka[2], Agnieszka Banas[3], Krzysztof Banas[3], Mariusz Gajda[4], Grzegorz Dyduch[5], Wojciech M. Kwiatek[6], Mark B.H. Breese[3,7]

[1]Gabriel Narutowicz Hospital, Kraków, Poland
[2]School of Medicine in English, Jagiellonian University Medical College, Kraków, Poland
[3]Singapore Synchrotron Light Source, National University of Singapore
[4]Department of Histology, Jagiellonian University Medical College, Kraków, Poland
[5]Department of Pathomorphology, Jagiellonian University Medical College, Kraków, Poland
[6]Institute of Nuclear Physics PAN, Kraków, Poland
[7]Physics Department, National University of Singapore

Corresponding author: Bohdan Pawlicki, MD, PhD
ul. Sokola 52, 30-244 Kraków, Poland
Phone: +48 12 422 45 65; E-mail: bpawlicki@poczta.onet.pl

Abstract: O b j e c t i v e: The goal of this contribution is to present and familiarize the medical community with the method for the assessment of trace and essentials elements in prostate tissue sections.
M a t e r i a l s a n d m e t h o d s: X-ray fluorescence based technique (namely Synchrotron Induced X-ray Emission (SRIXE)) is described in terms of methodology, sample preparation and the evaluation of the recorded results (spectral data sets).
Materials for the samples were collected from the patients underwent radical prostatectomy due to *Adenocarcinoma prostatae*. Specimens were freeze-dried, cut by microtome (to the thickness of 15 μm), one slice was placed on Mylar foil (for SRIXE measurements) and adjacent one on microscopic glass (for histopathological assessment).
R e s u l t s: Results presented here show the usability of SRIXE method for the evaluation of concentration of trace and essential elements in prostate tissue sections with the spatial resolution better than 15 microns.
D i s c u s s i o n: Histopathological analysis of samples, which is only focused on morphological features, is unable to reveal information about changes in biochemical signature of tissues affected by the illness. SRIXE is a powerful and promising technique to analyse even very low concentrations of selected elements

at the cellular level without any labelling or separating procedures. Obtained results may be correlated with classic histopathological assessment allowing for drawing conclusions on the changes in certain elements concentrations with the progression of disease. Moreover, mentioned in this work analysis, can be performed for any type of biological tissues.

Key words: prostate, SRIXE, trace elements, elemental analysis, X-ray Fluorescence, *Adenocarcinoma prostatae.*

Introduction

Biological point of view

Adenocarcinoma prostatae is one of the most repeatedly occurred cancer among men and one of the primary causes of death. According to statistics [1], an estimated 1.11 million men were diagnosed with prostate cancer in 2012, with incidence rates varying 25-fold across the world. Discrepancies in incidences of prostate cancer are connected to availability of screening for prostate-specific antigen (PSA) and subsequent biopsies; the highest numbers are reported for countries with higher socioeconomic development.

Most prostate cancer cases (92%) [2] are detected at rather early stage, what means that the disease is restrained only to prostate gland and its near proximity organs. Early detection combined with properly designed treatment give higher chances for a man's individual long survival prognosis. It is of the utmost importance to gain access to all available information about the stage of the malignancy, prior to making a diagnosis. In addition to a physical examination, other important tests are taken into account: PSA (Prostate-Specific Antigen) and PCA3 tests, biomarker tests, transrectal ultrasound and eventually a biopsy that enables for definitive diagnosis (presence or absence of cancer). The Gleason score [3] is the widely used system for describing the prostate cancer stages for biopsy samples; the assigned scores show how far examined cells resemble the architecture of typical native (healthy) prostate cells. According to this system, the most well-differentiated tumors have a Gleason score of 1, and the least-differentiated tumors (generally more aggressive) a score of 4 or 5. The assessments are based on microscopic comparison of cells within examined section and usually are done by two histopathologists to avoid inaccurate classification. As this procedure relies mostly on what can be seen at the specific magnification, some biochemical information can be missed.

The causes of prostate cancer still remain unclear, so far researchers have found some risk factors which can escalate development of this type of malignancy [4, 5]. These risk factors include:

- age (prostate cancer appears usually in older man, the average age for positive diagnosis is about 66),

- race/ethnicity (for yet unknown reasons, the risk of prostate cancer is 74% higher in black men than in white men),
- family history (higher chances of finding this disease among men having brother or father with prostate cancer),
- gene changes (some of inherited genes can be involved in the prostate cancer progress),
- diet (higher risk of developing prostate cancer among men whose diet is rich with red meat, high-fat dairy products and calcium),
- obesity,
- smoking.

According to studies [6–8], it is also believed, that it may be direct link between concentration of selected elements and processes, which may transform healthy cells into cancerous ones.

Some of elements appearing in human body, only at the level of parts per million, drive very crucial chemical reactions being an essential components of biological enzymes; any discrepancies in their concentration may directly or indirectly be involved in cancerogenesis. Their presence at certain level may also indicate for an illness (cancer) progress.

Analysis of elemental concentration has become very popular in recent years. Nowadays, the scientists use many analytical techniques such as potentiometry, atomic absorption and emission spectrometry, X-ray and nuclear techniques [9] to analyse various types of samples including biological specimens. Taking into account their benefits and drawbacks, it seems that one of the physical methods called X-ray fluorescence (XRF) can "image" non-destructively concentration of various elements present in analysed samples at high spatial resolution providing information for better understanding of biomolecular processes occurring within the tissues. The sensitivity and accuracy of XRF depends mostly on the incident radiation energy, the efficiency of the detector and additionally the geometry of experimental set-up. It is worth adding that sample preparation is also very important step in the analysis.

Nomenclature

X-ray fluorescence (XRF) analysis is a very powerful multi-elemental analytical technique with plethora of applications to collect information about elemental composition of materials. XRF has gained a lot of attention especially in cases that require non-destructive analytical method.

An access to synchrotron radiation light sources, advancements in X-ray optics and detectors constructions, software and methodology for data analysis development have facilitated XRF application extension. Nowadays XRF analysis is not only focused on single spectra collection from selected region; very detailed two-dimensional maps

with a spatial resolution in the micrometer range can also be gained during **automatic or semi-automatic** experiments.

After reviewing available publications devoted to this topic [10–14], we noticed that XRF analysis performed with the help of synchrotron light sources is named differently in various contributions. Thus, there is a certain degree of ambiguity in the literature due to the fact that various names (and their acronyms) are used for naming exactly the same method. In order to clarify it, in the Table 1 these acronyms and their full names are summarized.

Table 1. Names of the method and acronyms used in the literature.

Acronym	Full name	References	Remarks
SRIXE	Synchrotron Radiation Induced X-ray Emission	[10, 11]	
SXRF	Synchrotron Induced X-ray Fluorescence	[12, 13]	
Micro-SRXRF	Microprobe Synchrotron Radiation X-ray Fluorescence	[14, 15]	
XFCMT	X-ray Fluorescence Computed Micro-tomography	[16]	for 2D/3D distributions of elemental concentrations
SRXRF	Synchrotron Radiation X-ray Fluorescence	[17]	

As the authors of this manuscript preference is the formulation: Synchrotron Radiation Induced X-ray Emission (SRIXE) this acronym will be used through this paper.

General idea

From the basic physics point of view, XRF may be described as the emission of fluorescent X-ray photons from a sample. This emission is also known as characteristic, as it contains information about elements existing within analysed area. Characteristic X-rays can be understood as a sample response to high-energy X-ray bombarding which leads to sample excitement (see Fig. 1).

Each element is described by its own electronic orbitals. As X-ray photons can carry enough energy to expel electrons from the atom inner orbitals; upon exposure to high energy photons ionization process may take place. One or more electrons are ejected from the atom only if the energy of radiation exposed to the atom is higher than its ionization energy. The removal of an electron from the inner orbitals leads to high instability in the atom electronic structure. The hole left by the expelled electron is filled within a very short time (around 100 fs) by the outer shell electrons. This process is accompanied by the creation of new secondary photon, which energy is equal to the energy difference between final and initial electron orbitals. To sum

up, exposed sample emits characteristic radiation allowing for the unequivocal identification of the elements present in it. In other words initial absorption of specific energy radiation results in the secondary emission of radiation of a different energy; thus, this whole process is called X-ray fluorescence.

This process is markedly useful for analysis of elemental contents hence is highly required in studies of ceramics, paintings, glass, alloys, construction materials, etc. Recently, this method has been also used for geochemistry, forensics and archaeological research, as well as life science applications including biological sample analysis.

In the textbooks, the main transitions are historically named as: K_α (transition between adjacent orbitals L and K), K_β (transition between M and K orbitals), L_β (transition between M and L orbitals), and so on.

The working principle of XRF technique is the wavelength or energy measurement along with the characteristic photon intensities emitted from the region of interest within analysed sample.

Collected fluorescent radiation is initially analysed by the calibration of the photons energies (so called energy-dispersive analysis). Once sorted, each characteristic radiation intensity is related straightforwardly to the concentration of the particular element in the sample.
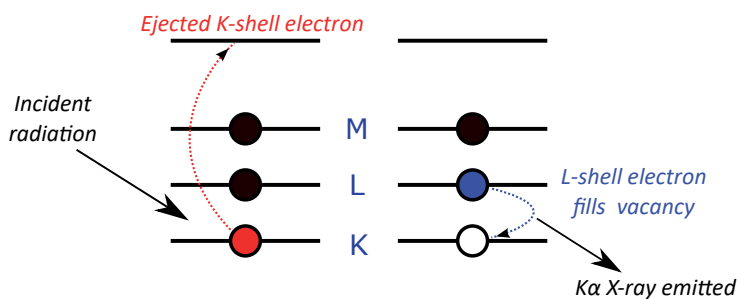

Fig. 1. Schematic presentation of X-ray fluorescence process.

Data, from the detector (namely the number of photon counts for each energy bin) is sent to the computer for the further analysis. The final output (XRF spectrum) — graph showing the number of photons for various energies after the results evaluation looks like the plot presented in Fig. 2. Measured spectrum contains peaks characteristic for electron transitions within atoms present in analyzed area of the sample. If concentration of selected element is high in the sample, K_α and K_β lines for this element are present in the spectrum. Essential part of the spectrum is called background; all peaks observed in the spectrum are "situated" above it. Background contribution represents all elastic and inelastic scattering of the primary radiation on the sample, as well as on substrate used to place not free-standing sample.

The quintessence of XRF analysis is the fact that, this technique enables the simultaneous qualitative and quantitative analysis of almost all elements (for light elements helium environment is required to allow low-energy fluorescence photons to reach the detector, for very heavy elements high energy of primary X-ray is required to excite the atoms).

To get the real concentrations of the elements, it is necessary to calculate the area under the peak corresponding to selected elements (after proper background subtraction), normalize these values to the incident photon flux and subsequently calculate efficiency curve (in order to convert calculated areas under the peaks into real concentration values) [18]. This method requires also collection of the spectra for multielemental standard samples (samples with known quantities of certain elements) exactly in the same geometry, as the main experiments were performed (external standard method).
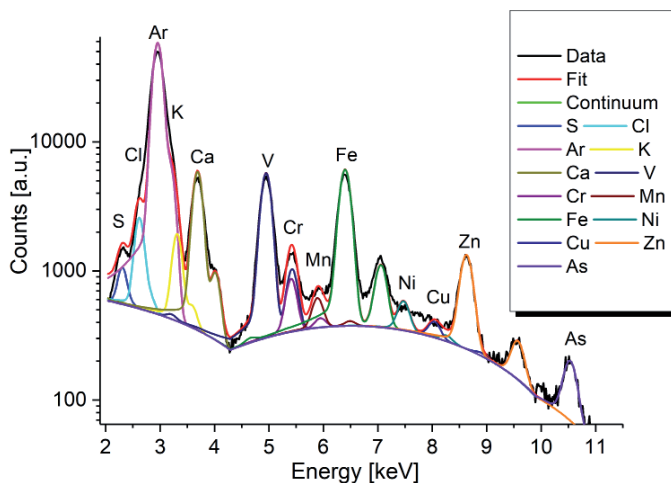

Fig. 2. SRIXE spectrum of the multi-elemental standard with deconvolution to the components (lines) related to specific elements.

There is also an option to calculate the concentrations from the first principles and geometric parameters of the setup, but usually it is less accurate than external standard method (due to the matrix and other effects).

To sum up, SRIXE is non-destructive analysis, has high accuracy and precision, can detect small amount of elemental concentration — from percent to ppm level (microgram per gram).

The goal of this paper is to present and familiarize the medical community with the method for the assessment of trace and essential elements in prostate tissue sections. Described here technique can be treated as a complimentary tool to histopathological

analysis of samples, which could shed additional light on the changes in biochemical signature of tissues affected by the illness. Accurate assessment of stage of the disease can contribute to highly dedicated treatment, which eventually can lead to extension of men's life. We do believe that presented here technique will become one day very useful for pathologists for more complete "diagnosis" of analysed sections.

Materials and methods

Samples description

Prostate tissue samples were collected from 12 patients (aged 56–72 years) underwent radical prostatectomies due to cancer diagnosis. Special attention was paid to sample preparation; the same protocol was used for all samples to minimize any potential contamination. Firstly, the materials were submerged in liquid nitrogen (−196°C) to halt all active processes taking place within cells, then they were cut with Leica ultramicrotome into slices of 15 μm thickness. Samples prepared for elemental analysis (SRIXE) were placed on Mylar foil (stretched on plastic frames) and left for air-drying. Mylar foil is one of the commercially available materials, widely used in XRF experiments, as it is thin (2.5 μm), transparent for X-rays and pure in terms of trace metal contamination. Adjacent sections assigned for histopathological examination were placed on microscopic glasses and stained later with hematoxylin and eosin (H&E) dye. As the final step, all samples were divided into groups according to Gleason grades.

Certain sections were selected for further SRIXE analysis; careful photographic documentation was made using Olympus BX-50 microscope. Example of chosen for SRIXE experiments area classified as Gleason 2+3 is depicted in Fig. 3.
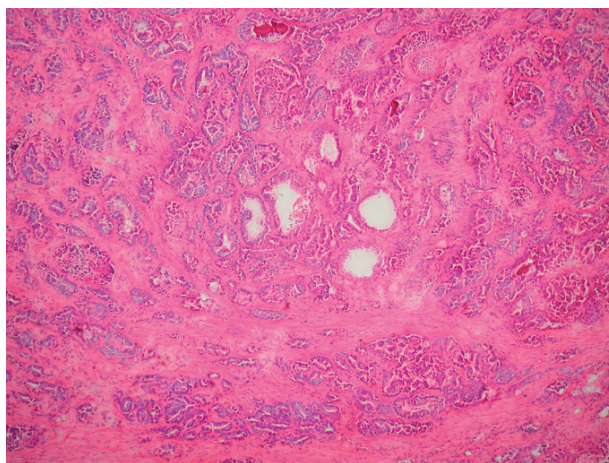

Fig. 3. Example of malignant cells within prostate tissue classified as Gleason 2+3. Photo depicts section stained with H&E; for SRIXE experiments, its adjacent section placed on Mylar foil was used.

Two multielemental gelatin standards, blend of selected metal (K, Ca, V, Mn, Fe, Zn, As, Pb, Sr, Zr, Mo) nitrates, were prepared to facilitate the assessment of concentrations of elements found within prostate tissue samples [18]. The metal concentrations in prepared reference standard samples were at the level of 10 μg/g, what was checked and confirmed by atomic absorption spectroscopy.

Setup description

SRIXE experiments were performed at the L beamline, one of the experimental stations at German synchrotron — the HASYLAB, DESY (Hamburg). Electron energy available at the Hasylab was equal 4.45 GeV, critical energy 16.04 keV, and maximum ring current ~120 mA.

Microprobe setup, available at beamline L, was highly used in multi-elemental analysis of micro-sized samples including biological sections. Greatly brilliant and linearly polarized synchrotron radiation (SR) was able to induce fluorescence for various elements having atomic numbers within 13–92 range (Al to U) with minimum detection limits down to 0.1 pg/μg [19].

Typically, experimental realization was the same as the one presented in Fig. 4. X-ray beam from the storage ring of the synchrotron was going through the polycapillary (14 μm in diameter), which was used to focus incoming radiation. Focussing means decreasing the size of the beam spot on the sample with preserving photon flux (keep as many photons as possible). As can be seen in Fig. 4, sample was
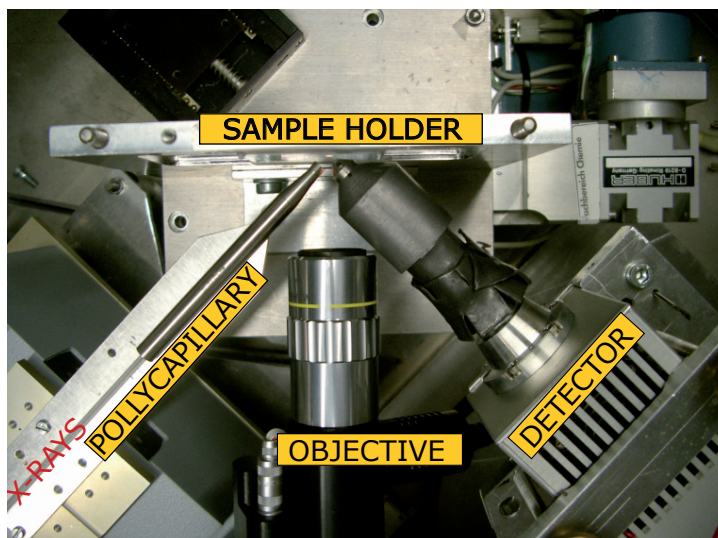

Fig. 4. Photography of the setup for SRIXE experiment.

placed very close to the polycapillary to keep the same size of the beam spot as the exit of the polycapillary (14 μm).

Energy dispersive detector (High Purity Germanium (HPGe)), capable of distinguishing the photons with various energies, placed at 90 degrees angle to the incoming beam, recorded the X-ray fluorescence photons emitted from the sample. Right angle between polycapillary and the detector was selected to minimize collection of the scattered X-ray photons. The detector energy resolution was equal to 140 eV for 5.9 keV. Sample was placed at 45 degrees angle in respect to detector and polycapillary, so that the path length of X-rays in the sample was minimized.

All experiments were carried out in the air. Position of the sample was being changed with micrometric precision by computer-controlled stepper motors. Microscope with a magnifications of 40 to 1200x allowed for remote selection of proper region of interest (ROI) within analysed sample. Additionally CCD camera with a resolution of 3 μm was used to monitor X-ray beam position on the sample. Time for single SRIXE spectrum collection was set to 5 mins; for chosen areas (even if they looked quite homogenous) several spectra were taken to obtain reliable and representative (for particular cells pattern) results.

Following details were saved during experiments: X-ray emission from particular spot, position of analysed spot, actual beam current of SR and the experimental time.

Results

Data evaluation techniques

After experiments performed at the L-beam line, all collected spectra were analysed by means of AXIL software working under Linux OS.

Fig. 5 shows the subsequent stages of data evaluation that lead from the recorded raw spectrum (number of photons recorded for each energy channel) to calculation the concentration of various elements present in the sample. First the energy calibration is applied that converts channel number of the detector to photon energy value (Fig. 5b), then spectrum is fitted with the model that incorporates information about energy position of main lines $K_\alpha, K_\beta, L_\alpha$; their relative amplitudes and distance lines for various elements as well as type of background function (Fig. 5c). Usually, procedure based on removal from the spectra rapidly changing points was used for background subtraction. From the fitted spectrum, it is possible to identify which elements are present in the sample (Fig 5d). Calculating the integral (area under the line-net peak area), is a crucial step to assess the relative concentration of the element (in Fig. 5e part of the spectrum with K_α and K_β for zinc is shown). In our analysis, net peak areas, normalized to the incident photon flux value, were used to estimate the concentrations of selected elements according to procedure described in [18].

a)

b)

c)

d)

e)
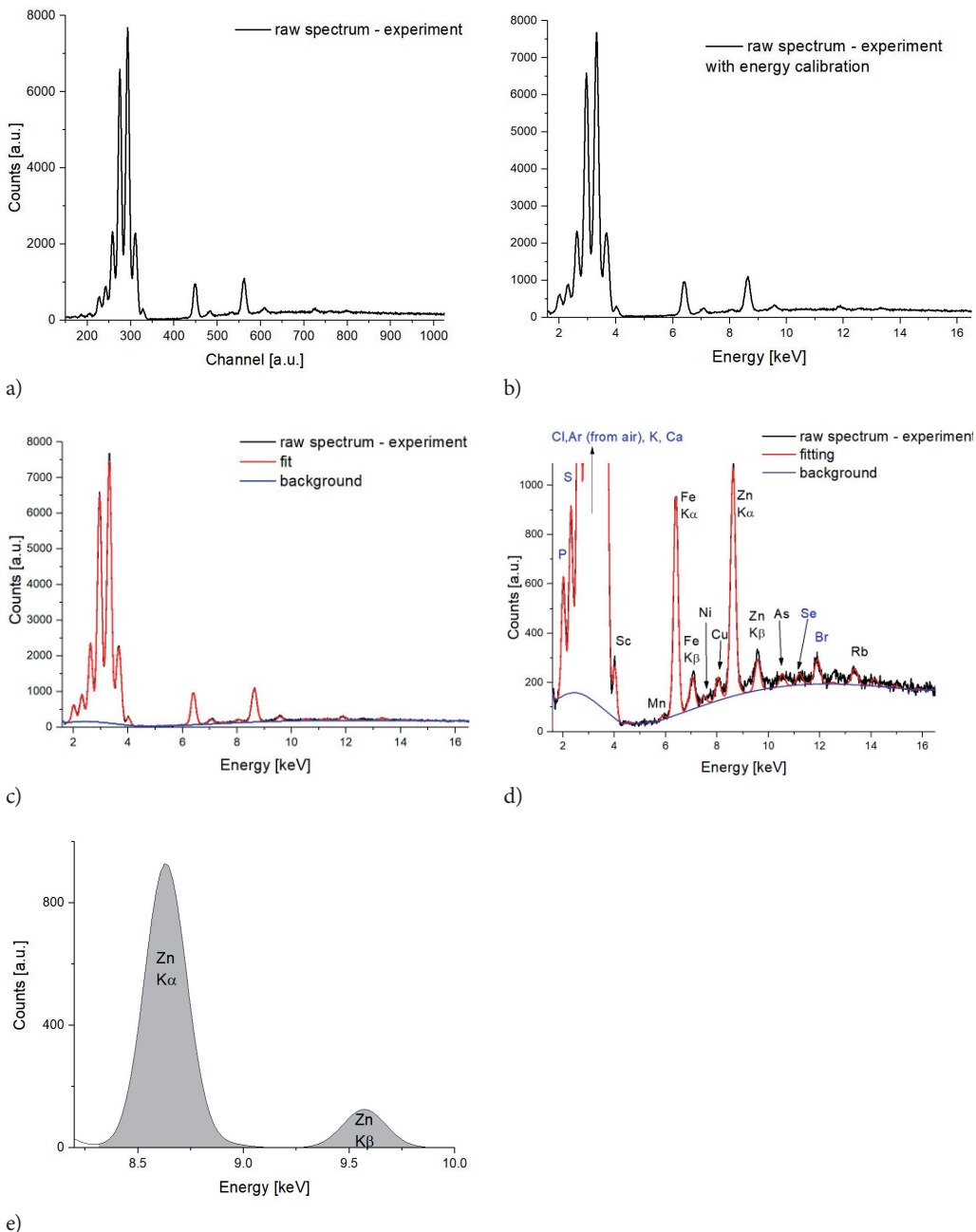
Fig. 5. Data processing on SRIXE spectrum: a — raw spectrum from the experiment: photon counts versus channel number; b — energy calibration; c — continuum (background) and spectrum fitting; d — assignment of the lines for particular elements; e — calculation of the integral (area under the peak that is proportional to the concentration).

Fig. 6 summarizes all steps required to obtain the concentration values for selected elements from measured SRIXE spectra.
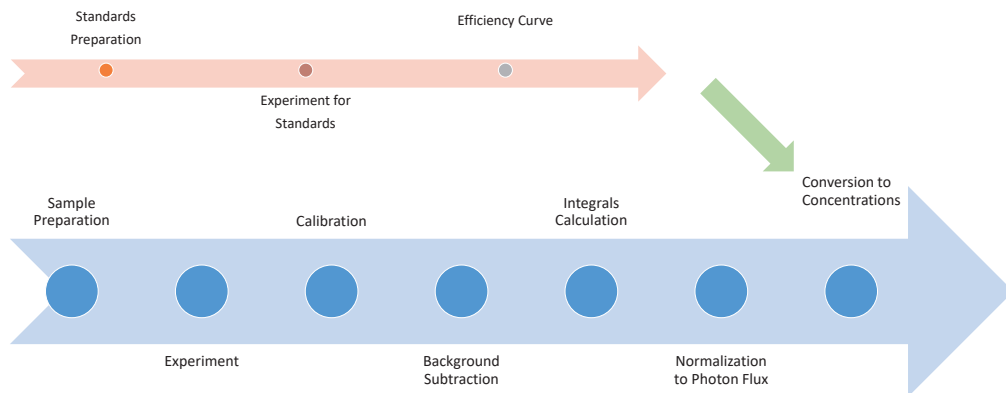

Fig. 6. Workflow for obtaining elemental concentrations based on the analysis of SRIXE spectra.

Graphic presentation and statistical analysis of obtained data were performed within R environment (version 3.4.2) [20] with R Studio (version 1.1.383) serving as graphic user interface (GUI). More than 300 SRIXE spectra were collected for samples classified as healthy, hyperplastic, Gleason grade 2 (GG2), Gleason grade 3 (GG3) and Gleason grade 4 (GG4). Descriptive statistical parameters (median, minimum and maximum, skeweness and curtosis) were computed for each elemental concentrations. For results discussion median values were chosen as all distributions of elemental concentrations were asymmetric and not normal (with $p < 0.05$).

In our studies, concentrations of subsequent elements: Ca, Cl, Cu, Fe, K, Mn, Ni, S and Zn were calculated; all of them play a vital role in maintaining the normal physiological functions in living organisms. As is presented in Fig. 7, their distributions differ among all analysed groups what may indicate that these elements are also involved in processes of turning healthy cells into malignant ones.

Box plots presented in Fig. 7 show that trend in distributions for Mn, Cu, Ni and Zn seem to be similar for selected groups; no significant differences can be observed for concentration median values between healthy and hyperplastic groups. However, for Gleason 2 group prominent increase in elemental concentrations can be noticed, for Mn this rise exceeds almost 10 times value found for healthy and hyperplastic groups. Elevated concentration level of these elements for Gleason 2 may be linked with accumulation of free radicals, which according to some studies [21–23] initiate biomolecular damage processes leading to many chronic health problems including cancer. The Fenton reaction may be catalysed by transition metals such as Mn and Cu.
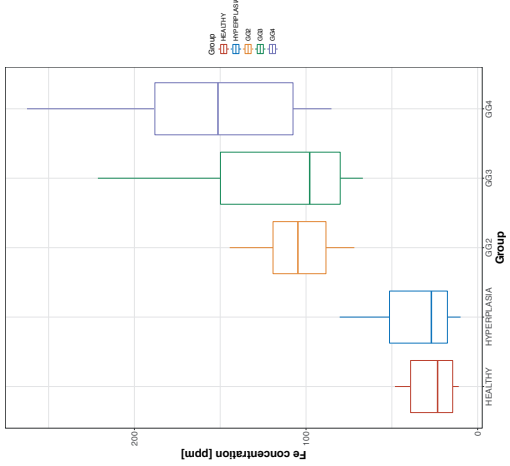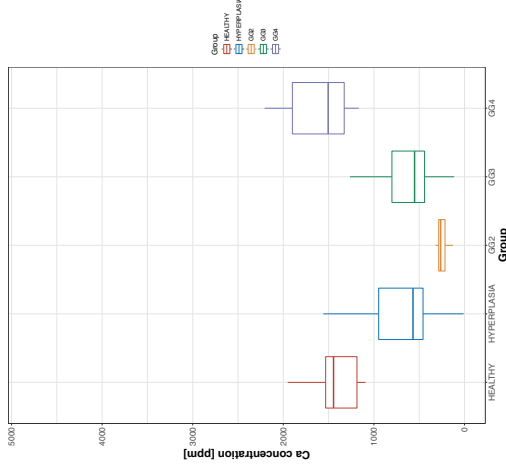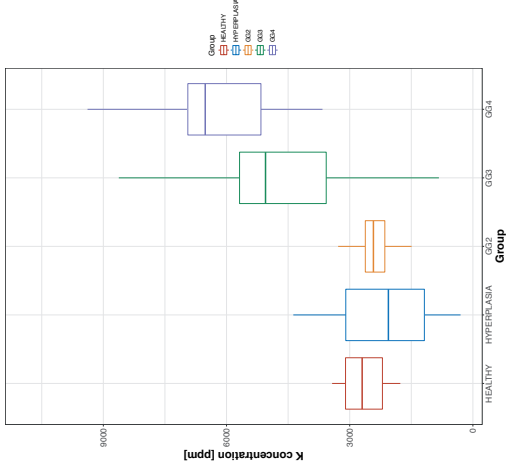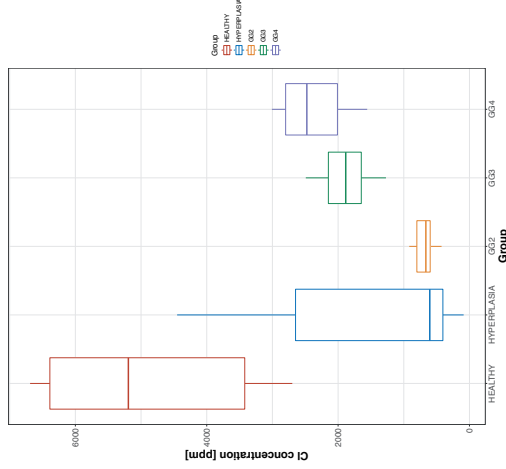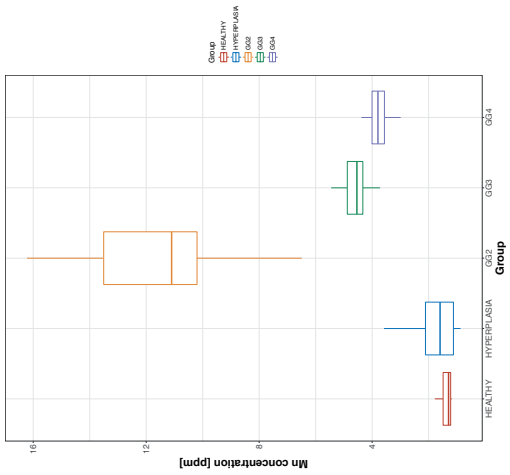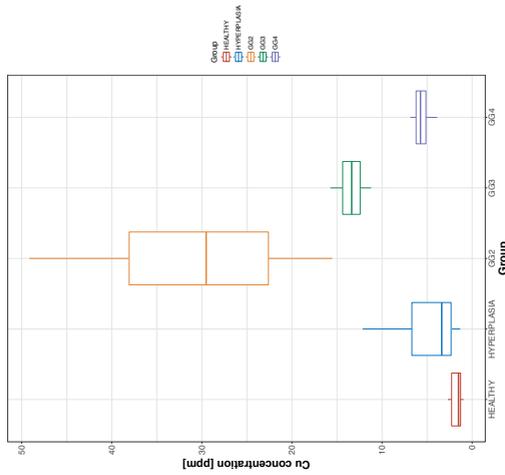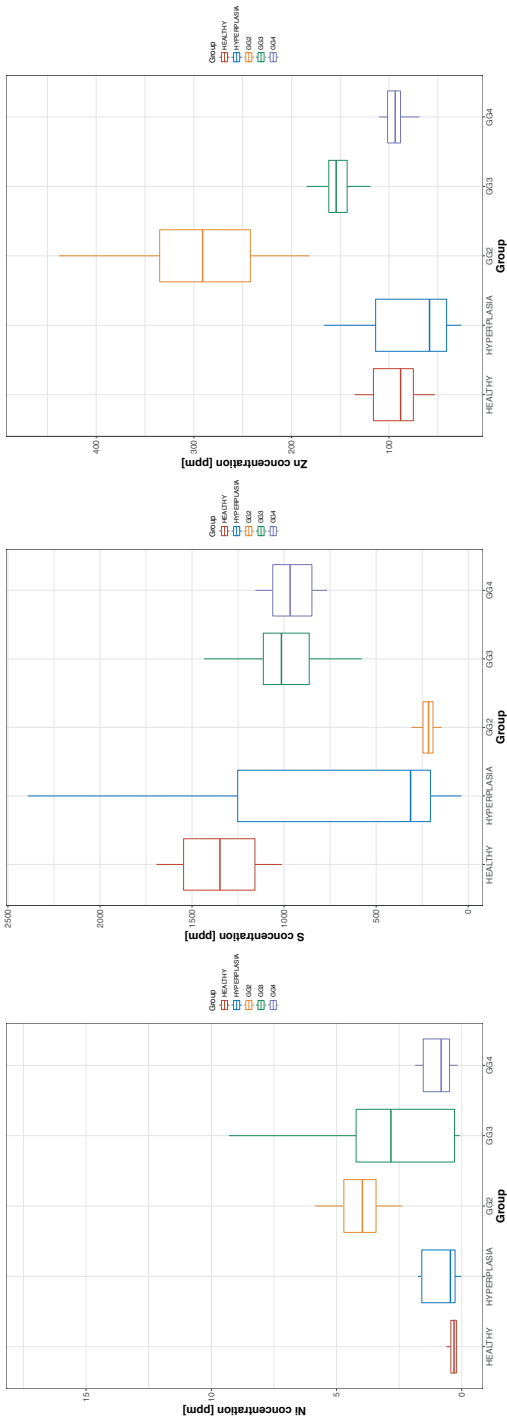
Fig. 7. Box plots representations of Ca, Cl, Cu, Fe, K, Mn, Ni, S and Zn concentrations [in ppm] across five groups (colour coded): healthy, hyperplasia, GG2, GG3 and GG4. The body of the box plot depicts the first and third quartiles of the distribution and the median line. The whiskers extend from the quartiles to the last data point within 1.5x interquartile range with outliers beyond.

Cu is also recognized as a switcher in turning on angiogenesis in tumor cells. Atypically high concentrations of Cu were found in serum of patients diagnosed with highly progressive tumors [24–26]. It is very likely that high level of Cu concentration in Gleason 2 may also be related to production of mechanism feeding the tumor — new blood vessels.

On the other hand Mn, Cu, Ni and Zn can play crucial role in the defence system against free-radicals being a part of superoxide dismutase, which catalyse the disproportionation of the cytotoxic superoxide radical (O_2^-) to hydrogen peroxide and molecular oxygen [27–29]. In our studies, we found diminishing quantities of these elements for more advanced stages of prostate cancer (Gleason 3 and 4 as compared to Gleason 2). Maybe this finding is somehow connected to a weakening in the defensive capability of cells.

As can be seen in Fig. 7, concentration distributions for Fe and K seem to follow another trend. In case of Fe, steady increase in concentrations is observed for more advanced cancer stage: about 3 times more for Gleason 2 and 3 and 6 times more for the Gleason 4 (with respect to the values obtained for tissues belonging to healthy and hyperplastic groups). This tendency may prove the fact that despite being essential for maintaining typical physiological tasks in human beings, Fe can be also involved in cancerogenesis via catalysis and generation of hydroxyl radicals from superoxide and hydrogen peroxide [30, 31] or working as a nutrient for microbial and malignant cells [32, 33].

Ca, K and Cl regulate many physiological functions of cells including their programmed death called apoptosis [34]. In our studies, elevated level of these elements can be observed for more advanced stages of cancerous tissues (Gleason 4 compared to Gleason 2).

S plays very important role in human body, mainly as a part of two amino acids, Fe-S clusters and gluthathion. Sulphur presence is critical for many cell processes including cell differentiation, proliferation, and apoptosis [35]. As it can be seen in Fig. 7 the highest value of median concentration for S is found in healthy group, for hyperplasia and GG2 groups decreasing trend is detected; but for more advanced cancer stages GG3 and GG4 again higher values are observed.

Conclusion

As it was mentioned in the introduction, pure histological analysis of biological samples, which is only focused on their morphological features, is rather incomplete, as it is unable to reveal information about changes in biochemical signature of tissues affected by the illness. As it is presented in this paper SRIXE technique is a powerful and promising method to analyse even very low concentrations of selected elements at the cellular level without any tedious and sophisticated sample preparation.

Analysis of SRIXE spectra can provide information of concentrations of elements that are present within tissue sections classified as healthy, hyperplastic and according to Gleason grading.

Based on our published papers [36–39], it can be concluded that concentration of selected, crucial for homeostasis, elements differ among analysed groups. However, their precise role in carcinogenesis is not very clear so far: are they promoter or antagonist in this process? It is known that some of elements can act as catalyzers of the Fenton reaction [40], or may be the part of prosthetic groups of several metalloenzymes such as superoxide dismutase, which is an important antioxidant enzyme in the cellular protection against reactive oxygen species [41].

It is worth stressing that information about chemical "status" of the analysed patterns defined by Gleason levels must be carefully processed. Single comparison of calculated median values of their concentration must by supported by appropriate chemometric analysis, which eventually may shed new light on the elucidation of complicated processes occurring within tissues during malignancy development.

The main goal of this paper was a short presentation of methodological approach for the elemental concentrations assessment in prostate tissue by SRIXE method. This technique may be also applied to analyse any other tissue sections. We do believe that information about concentration level of selected elements within various cancerous tissues combined with adequate statistical analysis can eventually open the way for not only understanding, but also for finding the new options of treatments which could prevent or slow down processes, which turn healthy cells into malignant ones.

Funding

Conflict of interest

No declared.

References

1. *Wong M.C., Goggins W.B., Wang H.H., Fung F.D., Leung C., Wong S.Y., Ng C.F., Sung J.J.*: Global Incidence and Mortality for Prostate Cancer: Analysis of Temporal Patterns and Trends in 36 Countries. Eur Urol. 2016; 70 (5): 862–874.
2. http://www.cancer.net/cancer-types/prostate-cancer/statistics.
3. *Gleason D.F.*: Histological grading and clinical staging of prostatic carcinoma. In: Tannenbaum M., ed. Urologic Pathology: The Prostate. Lea &Feibiger, Philadelphia 1977; 171–98.

4. *American Cancer Society*: Cancer Facts & Figures 2016. Atlanta, Ga: American Cancer Society; 2016.
5. *Nelson W.G., Carter H.B., DeWeese T.L., Antonarakis E.S., Eisenberger M.A.*: Prostate cancer. In: Abeloff's Clinical Oncology. Eds. J.E. Niederhuber, J.O. Armitage, J.H. Doroshow, M.B. Kastan, J.E. Tepper. 5th ed. Elsevier Saunders, Philadelphia, PA 2014; chap 84.
6. *Navarro Silvera S.A., Rohan T.E.*: Trace elements and cancer risk: a review of the epidemiologic evidence. Cancer Causes Control. 2007; 18 (1): 7–27.
7. *Schwartz M.K.*: Role of trace elements in cancer. Cancer Res. 1975; 35: 3481–3487.
8. *Adeoti M.L., Oguntola A.S., Akanni E.O., Agodirin O.S., Oyeyemi G.M.*: Trace elements; copper, zinc and selenium, in breast cancer afflicted female patients in LAUTECH Osogbo, Nigeria. Indian J Cancer. 2015; 52 (1): 106–109.
9. *Brown R.J.C., Milton M.J.T.*: Analytical techniques for trace element analysis: an overview. Trends in Anal. Chem. 2005; 24 (3): 266–274.
10. *Jones K.W., Berry W.J., Borsay D.J., Cline H.T., Conner W.C., Fullmer C.S.*: Applications of Synchrotron Radiation–Induced X-Ray Emission. (SRIXE). X-Ray Spect. 1997; 26: 350–358.
11. *Banas A., Kwiatek W.M., Zajac W.*: Trace element analysis of tissue section by means of synchrotron radiation: The use of GNUPLOT for SRIXE spectra analysis. J Alloys Compd. 2001; 328 (1–2): 135–138.
12. *Ryan C.G., Etschmann B.E., Vogt S., Maser J., Harland C.L., Van Achterbergh E., Legnini D.*: Nuclear microprobe — Synchrotron synergy: Towards integrated quantitative real-time elemental imaging using PIXE and SXRF. Nucl Instrum Methods Phys Res B. 2005; 231 (1–4): 183–188.
13. *Punshon T., Ricachenevsky F.K., Hindt M.N., Socha A.L., Zuber H.*: Methodological approaches for using synchrotron X-ray fluorescence (SXRF) imaging as a tool in ionomics: examples from Arabidopsis thaliana. Metallomics. 2013; 5 (9): 1133–1145.
14. *Uzonyi I., Szoor G., Vekemans B., Vincze L., Rozsa P., Szabo G., Somogyi A., Adams F., Kiss A.Z.*: Application of combined micro-proton-induced X-ray emission and micro-synchrotron radiation X-ray fluorescence techniques for the characterization of impact materials around Barringer Meteor Crater. Spectrochim. Acta, Part B. 2004; 59 (10–11): 1717–1723.
15. *Wang Y., Specht A., Liu Y., Finne L., Maxey E., Vogt S., Zheng W., Weisskopf M., Nie L.H.*: Microdistribution of lead in human teeth using microbeam synchrotron radiation X-ray fluorescence (μ-SRXRF). X-Ray Spectrom. 2017; 46 (1): 19–26.
16. *Simionovici A., Chukalina M., Gunzler F., Schroer C., Snigirev A., Snigireva I., Tummler J., Weitkamp T.*: X-ray microtome by fluorescence tomography. Nucl Instrum Methods Phys Res A. 2001; 467–468: 889–892.
17. *Radtke M., Reinholz U., Gebhard R.*: Synchrotron Radiation-Induced X-Ray Fluorescence (SRXRF) analyses of the Bernstorf Gold. Archaeometry. 2017; 59 (5): 891–899.
18. *Kwiatek W.M., Hanson A.L., Paluszkiewicz C., Gałka M., Gajda M., Cichocki T.*: Application of SRIXE and XANES to the determination of the oxidation state of iron in prostate tissue sections. J Alloys Compd. 2004; 362: 83–87.
19. *Falkenberg G., Clauss O., Swiderski A., Tschentscher T.*: Upgrade of. F fluorescence beamline at HASYLAB/DESY. X-ray Spectrom. 2001; 30: 170–173.
20. *R Development Core Team*: The R project for statistical computing. 2017; http://www.r-project.org.
21. *Machlin L.J., Bendich A.*: Free radical tissue damage: protective role of antioxidant nutrients. FASEB J. 1987; 1: 441–445.
22. *Armendariz A.D., Vulpe C.D.*: Nutritional and genetic copper overload in a mouse fibroblast cell line. J Nutr. 2003; 133: 203–282.
23. *Rae T.D., Schmidt P.J., Pufahl R.A., Culotta V.C., O'Halloran T.V.*: Undetectable intracellular free copper: the requirement of a copper chaperone for superoxide dismutase. Science. 1999; 284: 805–808.

24. *Folkman J.*: What is the evidence that tumors are angiogenesis dependent? J Natl Cancer Inst. 1990; 82: 4–6.

25. *Brem S.*: Angiogenesis and cancer control: from concept to therapeutic trial. Cancer Control. 1999; 6: 436–458.

26. *Hu G.*: Copper stimulates proliferation of human endothelial cells under culture. J Cell Biochem. 1998; 69: 326–335.

27. *Shearer J.*: Insight into the Structure and Mechanism of Nickel-Containing Superoxide Dismutase Derived from Peptide-Based Mimics. Acc Chem Res. 2014; 47: 2332–2341.

28. *Macmillan-Crow L.A., Cruthirds D.L.*: Invited review: manganese superoxide dismutase in disease. Free Radic Res. 2001; 34: 325–336.

29. *Zowczak M., Iskra M., Paszkowski J., Manczak M., Torlinski L., Wysocka E.*: Oxidase activity of ceruloplasmin and concentrations of copper and zinc in serum of cancer patients. J Trace Elem Med Biol. 2001; 15: 193–196.

30. *Rice-Evans C., Burdon R.*: Free radical-lipid interactions and their pathological consequences. Prog Lipid Res. 1993; 32: 71–110.

31. *McCord J.M.*: Iron, free radicals, and oxidative injury. Semin Hematol. 1998; 35: 5–12.

32. *Weinberg E.D.*: The role of iron in cancer. Eur J Cancer Prev. 1996; 5: 19–36.

33. *Toyokuni S.*: Role of iron in carcinogenesis: cancer as a ferrotoxic disease. Cancer Sci. 2009; 100: 9–16.

34. *Dubois C., Vanden Abeele F., Prevarskaya N.*: Targeting apoptosis by the remodelling of calcium--transporting proteins in cancerogenesis. FEBS J. 2013; 280 (21): 5500–5510.

35. *Czapla J., Kwiatek W.M., Lekki J., Steininger R., Gottlicher J.*: Determination of changes in sulphur oxidation states in prostate cancer cells. Acta Phys Pol A. 2012; 121 (2); 497–501.

36. *Banas A., Kwiatek W.M., Banas K., Gajda M., Pawlicki B., Cichocki T.*: Correlation of concentrations of selected trace elements with Gleason grade of prostate tissues. J Biol Inorg Chem. 2010; 15: 1147–1155.

37. *Banas A., Banas K., Kwiatek W.M., Gajda M., Pawlicki B., Cichocki T.*: Neoplastic disorders of prostate glands in the light of synchrotron radiation and multivariate statistical analysis. J Biol Inorg Chem. 2011; 16 (8): 1187–1196.

38. *Banas K., Jasinski A., Banas A.M., Gajda M., Dyduch G., Pawlicki B., Kwiatek W.M.*: Application of linear discriminant analysis in prostate cancer research by Synchrotron Radiation–Induced X-Ray Emission. Anal. Chem. 2007; 79: 6670–6674.

39. *Banas A., Banas K., Falkenberg G., Dyduch G., Pawlicki B., Kwiatek W.M.*: Using micro-synchrotron radiation induced X-ray emission distribution maps to determine correlation between elements in prostate tissue. Spectrochim Acta, Part B. 2008; 63: 957–961.

40. *Bokare A.D., Choi W.*: Review of iron-free Fenton-like systems for activating H2O2 in advanced oxidation processes. J Hazard Mater. 2014; 275: 121–135.

41. *Halliwell B.*: Reactive Species and Antioxidants. Redox Biology Is a Fundamental Theme of Aerobic Life. Plant Physiol. 2006; 141 (2): 312–322.